IJBPAS, November, Special Issue, 2021, 10(11): 1024-1038
ISSN: 2277–4998

International Journal of Biology, Pharmacy and Allied Sciences (IJBPAS)
'A Bridge Between Laboratory and Reader'

www.ijbpas.com

DEEP LEARNING APPROACH FOR DENOISING CONTOURS AND CLASSIFICATION OF AUTOMATIC HEALTH TISSUE IMAGE WAVELETS VIA CNN

NEHA GAUTAM[1*], POORNIMA H. N[2], B BUVANESWARI[3], KUMAR R. G[4], CHANDRA SEKHAR KOPPIREDDY[5] AND SONU KUMAR[6]

1: Faculty of Engineering & Technology, JAIN (Deemed-to be University), Bengaluru, Karnataka

2: Research Scholar in Information Science at AMC College of Engineering, Bangalore, Karnataka, India

3: Professor, Department of Information Technology, Panimalar Engineering College, Chennai, Tamil Nadu, India

4: Associate Professor, Department of CSE, Siddharth Institute of Engineering & Technology, Puttur, Andhra Pradesh - 517583, India

5: Assistant Professor in Computer Science and Engineering at Pragati Engineering College, Surampalem, East Godavari, Andhra Pradesh

6: National Level Coordinator, Ignite, Bhumi, Chennai, Tamil Nadu

***Corresponding Author: Neha Gautam; E Mail: nehagautam1208@gmail.com**

Received 23rd July 2021; Revised 27th Aug. 2021; Accepted 30th Sept. 2021; Available online 1st Nov. 2021

https://doi.org/10.31032/IJBPAS/2021/10.11.1088

ABSTRACT

Image classification is crucial in diagnostic scanning, notably when combining architectural pictures from CT, MRI, and operational pictures from photonic techniques or various new image analysis methods. Whenever combined using 3D photon transportation simulations techniques, picture separation additionally offers precise anatomical descriptions enabling quantified depiction of the therapeutic photon dispersion as in the body. Using five MRI face imaging files, we firstly employ post approaches like polynomial conducting to recover the precise outlines of distinct components including the cranium, cerebral liquid

(CSF), grey material (GM), and grey material (WM). They then use a multilayer neuronal network to achieve automated picture identification employing machine knowledge. Concurrent computation is also covered. When opposed to hand or automation separation, such techniques significantly lowered processor times and are critical for boosting performance and reliability as additional examples are learned. The algorithm counts the overall quantity of separated Gray and whitish material information, indicating that this fragmentation method can objectively diagnose brain degeneration. We show how photosynthesis and machine intelligence coupled with automated tissues imaging categorization may be very useful in neurologist surgery.

Keywords: Deep learning; Artificial intelligence; Convolutional neural network; Brain image wavelet; Denoising Contour; Health tissue

INTRODUCTION

The picture of grey matter produced by radioactive magnets' radiation scanning is crisp and elevated. It is a typical approach for examining cerebral disorders clinically. The anatomy of the neural network is extremely complex. Forebrain, brain volume, or subarachnoid fluids are all significant structures. Remembering, intellect, consciousness, and speech are all aided by these cells **[1]**. According to fuzzy borders, critical components including cerebral fluids, nerve fibers, or brain structures are difficult to distinguish. Therefore, clinicians have a difficult time studying these independently and pinpointing cancer's site **[2]**.

Computer-assisted clinicians may increase the effectiveness of fragmenting the grey and white material of the cerebral MRI **[3]** as graphics clinical treatment becomes more common. Various signals strengths or balanced imaging (T1 and T2 stacked) might cause the picture to show as variable grey tones in MR scanning. The investigation chooses to use a cerebral radiofrequency T1-W picture for a research specimen because its T1 brain magnetism picture reveals that the tendons are stronger **[4-6]**.

Numerous attempts had been undertaken to dynamically partition the brain picture. Straightforward though ineffective segmented methods depending on region, topological, and statistic criteria exist. Sensitivity is a basic yet efficient method of picture segmentation **[7]**. Nonetheless, they are significant drawbacks to employing such an approach only for separation **[8]**. To begin with, the grey scaling of organs may not be limited to a single spectrum. This indicates that if we just employ a baseline to find the organs,

we might not be able to differentiate all of them **[9]**. Furthermore, the minimum will rarely generally consider a picture's geometric characteristics **[10]**. The cranium, for one, is a spherical framework that protects the surrounding organs. That could assist us in determining organ placement and obtaining highly precise segmented pictures. As a reason, thresholding is frequently seen as a first-stage sequencing picture procedure **[11]**.

Literature survey

Further on, clustering and machines intelligence approaches were discussed. Regarding head imaging extraction, the classification approach is particularly frequently employed. It has a computer foundation that is rather sophisticated **[12]**. Nevertheless, in addition for obtain reliable findings, precise knowledge of amplitude and topological characteristics is necessary. Convolutional neuronal systems might be used to ignore vertical and amplitude information. Another deeper controlled teaching approach was the convolutional brain networks. It's being used in a variety of disciplines, with notable results in picture detection, audio recognition, and spoken word synthesis **[13]**. Using circular compression combining sampling with an unsupervised learning method, CNNs derive the combination strength **[14]**. The ultimate simulation is obtained immediately from the source, which is advantageous to the classifying characteristics. Material, form, & architecture were key elements used in picture identification.

Using five MRI brain imaging collections, they employ picture enhancing, operations, and morphological approaches to recover precise outlines of distinct regions. Then, employing profound intelligence, we use a multilayer neuronal network to achieve automated picture classification. When compared with previous technologies, those techniques significantly decreased computing times. Use concurrent computation to boost down overall working rate even that far. Inside this healthcare area, our research has a lot of promise for detecting brain illness.

MATERIALS AND METHODS

The brain MRI T1-W scans of five participants are included in the collection. You possess 160 pictures for each subject, for a maximum of 800 photographs. The pictures are 256 x 256 bytes in dimension. This matrix's pixels values are all integers among 0 and 255. A common MRI of a neural network is shown in **Figure 1**. Any MRI information used to corroborate the conclusions of this investigation may be obtained by contacting the respective researcher.

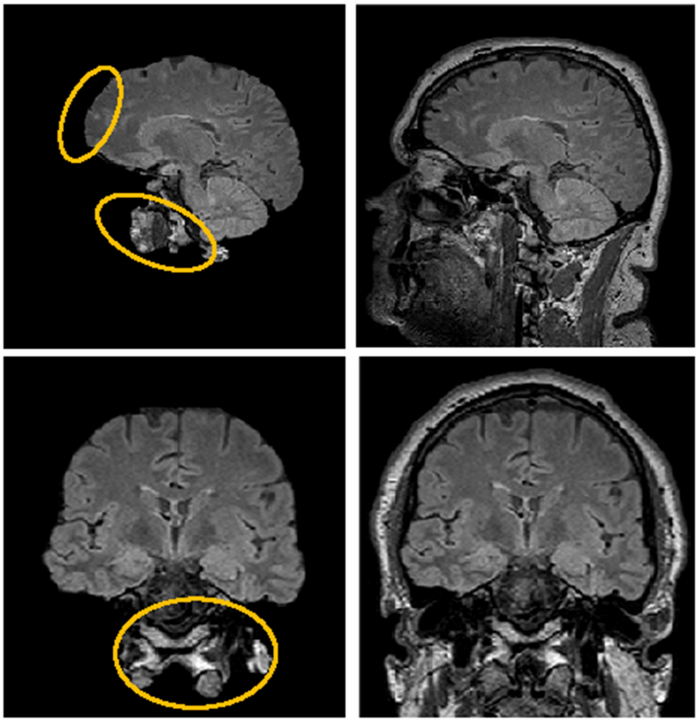

Figure 1: MRI Images of Skull

There are numerous overlapped areas in every MR picture because of the body's interconnected nature. The picture which was before can enhance the individual's effectiveness as well as the accuracy of the classification outputs. Visual noise removal and improvement could help it's visual correspond to the viewer's expectations **[15]**. You may prevent a colorful cranium from interfering with the brain's classification quality by eliminating it. Photo distortion removal has a strong impact on categorization results. Spectral domains data reduction employs multiresolution conversion to convert chaotic data between the temporal domains to the curvelet sector. For the fractal components from information, eliminated those fractal components of disturbance across all dimensions. Eventually, a nonlinear technique is used to reconstitute the waveforms. The snapshot with distortion suppression retains the underlying article's features and improves the aesthetic impression **[16]**. To improve the picture of the intracranial fluids, nerve fibers, and subcortical white, the gaussian balancing approach is employed.

When demonstrated by **Figure 2**, they gathered the greyish levels of all 800 MRI pictures and created a distribution that included all the spots. The data reveals four maxima, every representing a different type of tissue. The number, which was lower than 35, cannot reveal its backdrop greyish tone. Images that are outside in the

greyscale region of the GM, WM, CSF, and cranium can be removed using the spectrum. To decrease overall cacophony, we set each to degree 0. The 4 boundaries in the distribution represent the 4 organs **[17]**. We appear to be able to partition the picture solely based on this finding. These are, nevertheless, certain limitations. Cut-off seldom analyses a picture's geometric characteristics. Its cranium, for particular, has a spherical form that is situated surrounding another organ. Furthermore, a tissue's greyish grade might not be confined to a single area. Dependent upon your environment, the greyish quantity of GM may be in the CSF. As a consequence, relying solely on the boundary in primary analytical gauging methodology might never yield correct results.

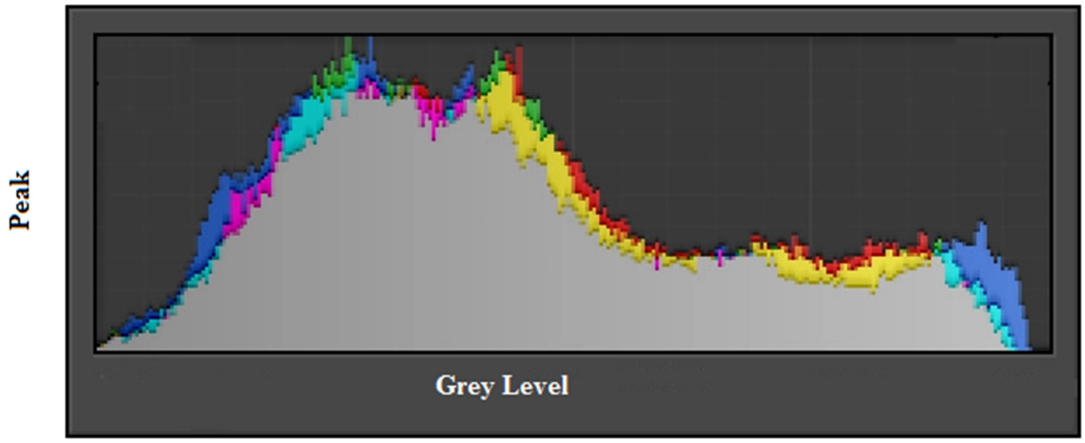

Figure 2: Histogram of cerebrospinal fluid

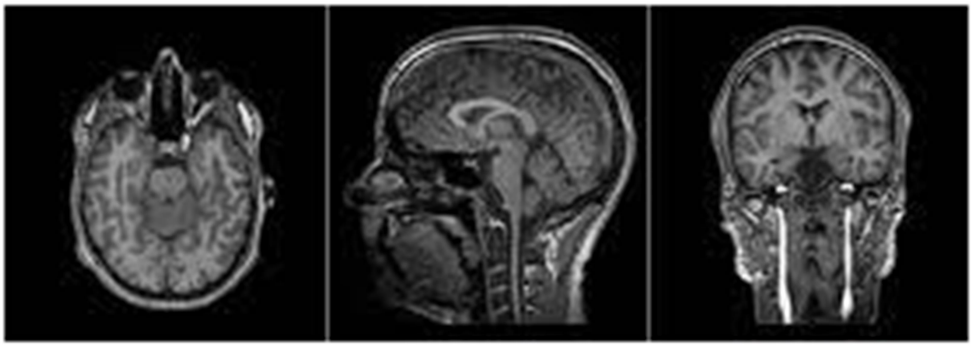

Figure 3: Patients Cross-Sectional Brain image sample

CNN

For picture identification & separation, recurrent neuronal systems (CNNs) have lately seen a lot of successes. CNN's have 2 levels in their fundamental construction shown in **Figure 3**. This features separation layers were 1 of them (C1, C3). Every photoreceptor input is linked to the preceding gradient localized responsive region, which extracts the

localized property. The spatial connection among a localized component and that remainder may be established after it has been recovered **[18]**. That pattern matching networking plane is the opposite level (S2, S4). Numerous features mapping makes up every computational level. The characteristic mapping is a uniform surface with identical values for every neuron. A perceptron for the convolutional network in the information translation framework is the stochastic value. Furthermore, since a neuron on a translation surfaces shares values, the quantity of unbound variables in the system is decreased. With this CNN, every recurrent layer is soon followed by a computational structure for the regional averaging and subsequent retrieval. Overall component quality is reduced thanks to the one-of-a-kind extractor architecture.

This C3 level was likewise another convoluted structure that convolutes the level Switches with input baseline value 5 x 5. There are just 10 transistors on the features mapping, yet there are 16 distinct convolutional cones. As a result, there were 16 characteristic mappings in all. Every picture in C3 is made up of all 6 or multiple highlight mappings from S2. These partial connecting techniques maintain the amount the interconnections inside an acceptable level, thus you don't attach every feature mapping of overall S2 to C3. Furthermore, it breaks the channel's balance. The fact that various featured mappings contain distinct outputs causes companies the recover distinct aspects that push them to recover distinct characteristics. The S4 level is a features image pooled level made up of sixteen 5x5 sized featured mappings. So, the similar way that both C1 or S2 features maps are attached to that 2x2 community for its matching characteristic mapping there so C3, every item of that featured mapping is attached to the 2x2 community of the associated characteristic mapping in the C3. This F6 level was entirely linked with the Cyclin level which contains 84 subunits. Ultimately, the outputs level is made up of a Geometric zonal base functional unit having 84 sources per unit.

This convolutional gradient result comprises the combination of the convolutional code and the higher gradient result:

$$a = e\left(\sum_{j=N} a^1 * l^1 + y^1\right) \qquad (1)$$

$$a = e(\beta^1 down\,(a^1) + y^1) \qquad (2)$$

Its CNN's characteristics were configured as regards **Figure 4**. This neuronal network is coordinated across 3 strands: the incoming level contains numerous 4x4 image values, the compression phase contains six 3x3 kernel values, and the bottom level contains six

2x2 image components. Eventually, following retraining, the variables of the robust networks were acquired. There were numerous 2D plane components within every level, and every 2D plane component has numerous individual synapses. The deeper features information is extracted because the result comprises 6 images. Regarding our teaching technique, we employed the Adams algorithms. Our starting acquisition rate was fixed at 0.001 while its current was set to 0.5. For a cost function, we employed crossing permeability. The CNN was educated over a period spanning 50 periods, every with 20 periods. The number of people in your group is 5. Learning examples are chosen at randomness amongst a minimum of 800 pictures: 600 photographs are used for learning, 100 for validity, and 100 for assessment.

Numerous parallelization computer architectures use MPI as their foundation. They employed an MPI-compliant Caffe platform. This MPI allows the clustering edition of Caffe to analyze information concurrently. It has a mission, Python, and MATLAB clients, as well as a variety of development approaches. Intel(R) Xeon(R) CPU E5-2670 0 @ 2.60 GHz represents typical Processor specifications. You combine the 800 arrays onto a single big column of the dimensions 800x65536. A row for inserting the picture identification was also included. This column represents one picture. The picture's reference was each initial integer on every row. All picture information is compiled into a single vector. As a result, all the pictures are processed at the same moment. The maestro paradigm is used. It consists of 2 procedures: the master's microprocessor is responsible for completing task instructions, and its assistant computer is the responsibility of assisting to master's compiler. The apprentice processors carry out the tasks that the masters processing allocates to it.

Each node serves as its primary server in this system because it is accountable for information partitioning and distribution. Then additional networks finish the regional information computation and send the results to the parent station. Figure 6 shows that the supervisor network receives the information and allocates it to the additional units before selecting the planet's core. The learners compute the separation around every location with that information building's middle, next record every node is grouping, estimate the total all that ranges among all the locations for every cluster and the planet's facility, and lastly report those findings to the masters. These clusters' locations represent the overall geographic dimensions of the

components in the GM, WM, CSF, and cranium. To properly identify the qualitative features of the distinct forms of information, you use the Proximity measure can determine the middle of the cellular component groupings, correspondingly, and select the criterion = 0.5, which removes 50% of information elements that are closest to the featured canter's locations. The central server would compute the current middle, communicate it to additional procedures, then finally estimate its opposite processing from the grouping of all locations to the summation of the distance's canters. That procedure will be repeated unless the total of all group lengths is consistently shown in **Figure 5**.

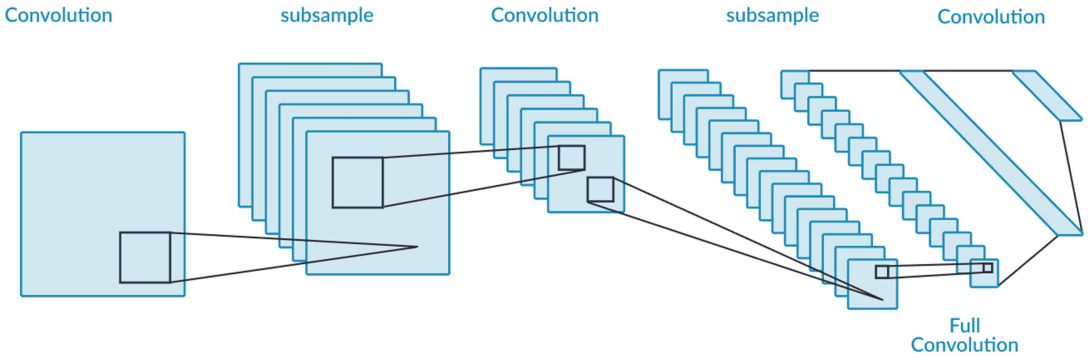

Figure 4: Proposed Structure of CNN

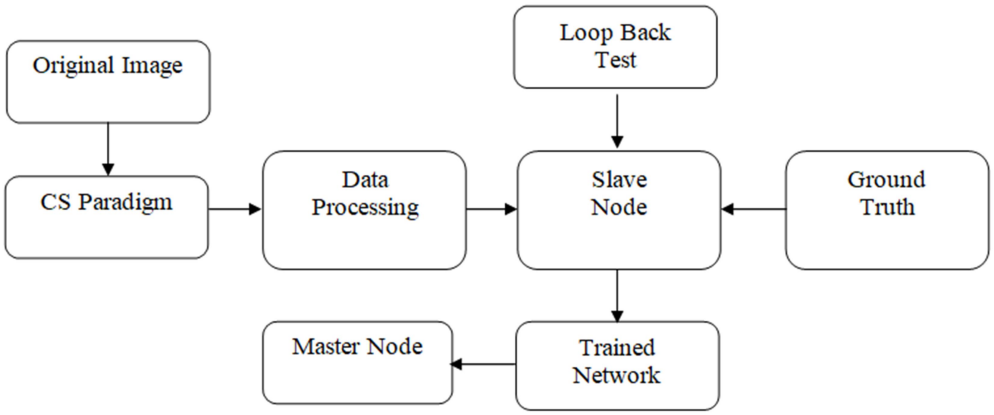

Figure 5: The master-slave technique of parallel computing

RESULTS

5.1 Image Segmentation

Figure 6 depicts the outcomes of their research. These raw pictures may be found in the bottom columns. These display a comprehensive MRI imaging of the body's structures also well the various regions of the body including the facial bones, muscles, and hearing. They effectively segmented single brains picture

onto four photographs following eliminating the additional portions of the body which are deemed clutter. You adjusted the grey tone of the tissues to 255 and the backdrop to 0 for every picture.

The outcome of the helmet is a curving form placed on the body's border. Beneath the cranium and the greyish particulate mind is the cerebral fluids. The grey & brown material were likewise segregated precisely. They then conducted classification with pre-processing to see how effective the approach was. Their findings comprise a significant degree of disturbance from non-brain components well as the mouth, eyebrows, and various cosmetic features.

5.2 Comparative approach

These results were sensor contrasted to pictures separated by a professional operation. Researchers computed the proportion of every organ in the neural network and contrasted it to the transparent Mandarin person skull (VCH) models to quantify our findings. This physiological component was well represented by the VCH paradigm. It's primarily exploited in sunlight transmission simulations. Although the strength that sunlight fluctuates as it propagates, it can aid in calculating the number of cerebral regions. The VCH models were created using increased cryosection-colored images of an adult guy as a baseline. It consists of several sorts of materials taken from the corpse of an upright freezing guy. Their straight portion consistency is 0.02 cm, and the digitally colors picture quality is 0.01 cm for each pixel, this was stronger than CT and MRI. As a result, it's one of the more accurate skull simulations available, with accurate foldable geometries in the frontal brain.

Table 1 displays the information. Generally, we are pleased with our outcome. They can properly detect the border and separate the organs **Figure 7**. This percentage for greyish over whitish tissue was then computed and contrasted to the VCH finding, yielding a 95 percent agreement. That can be employed to diagnose disorders like brain degeneration, which is accompanied by a decrease in grey or white material. These are significant discrepancies between our findings and the reality. These are due to the residual disturbance and the computation inadequacy. Apart from cutting pictures, the MRI collection comprises slits pictures of the brains, showing display your entire skull more than just the mind. Therefore, the adjacent side of the brain would produce greater loudness. It also gives a generative logic for customers to determine the portion capacity, which is a useful approach to ensure that technology is

accurate shown in **Figure 8**. We contrasted their results to the VCH models, as well as several additional research, to determine the ratio of grey to whitish material. **Table 2** additionally includes the median findings. We also calculated the Jaccard index for each tissue, as shown in **Table 3**.

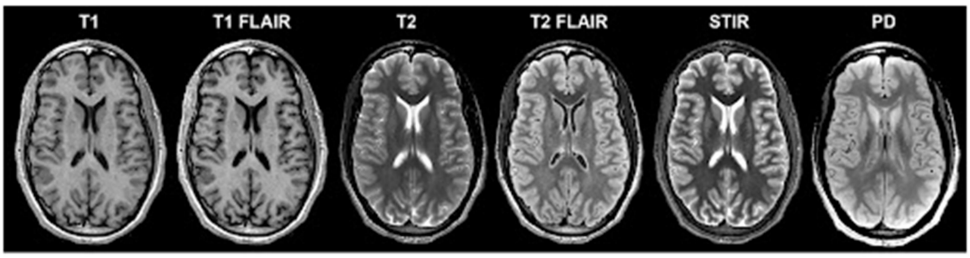

Figure 6: Images of Cerebrospinal fluid results

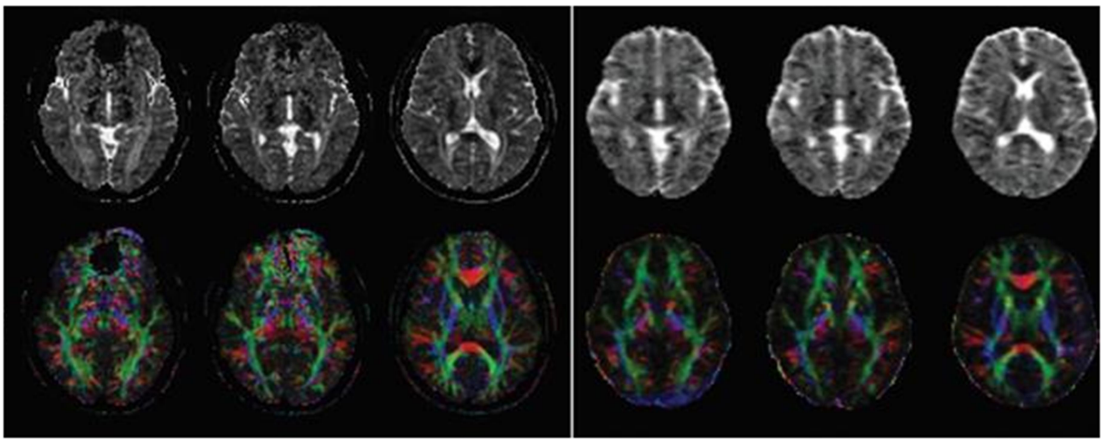

Figure 7: Comparison of different MRI scans

Table 1: The proportion of each tissue in the brain is compared

Classification	VCH in Percentage	MRI in Percentage
CSF	38	39 ± 2
GM	28	38 ± 1
WM	13	14 ± 0.8
Skull	13	12 ± 2

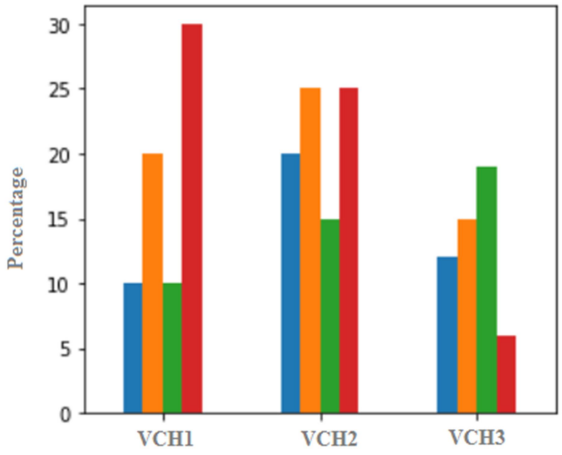

Figure 8: A comparison chart of Percentage of tissue and VCH result in brain

Table 2: The proportion of grey matter to white matter

Classification	Grey / White Matter
MRI	3.15
VCH	3.29
IS	3.08
Ge	2.2

Table 3: Four-tissue Iscard index

Classification	Index
CSF	0.85
GM	0.96
WM	0.97
Skull	0.82

On five MRI brain imaging collections, researchers employed imaging enhancements, operations, plus morphological approaches and derive precise outlines of 4 cells: the brain, cerebral liquid (CSF), parenchyma (GM), and whitish mind (WM). These multilayer brain networks are then used to do automated picture classification employing deeper knowledge. Spatial, texturing, and logarithmic thresholds techniques, as well as fuzzy c-means (FCM), have time consumption, precision, and resource constraints. The proportion of every organ is computed in our article, and this may be using it because a criterion for identifying illnesses like neurologic deficits, that is frequently triggered by grey material or whitish material decrease. They also employed simultaneous computation to cut down on the duration it took to complete the project.

That well before phase enhanced the individual's performance & both segmented result's dependability in the technique. Curvelet domains remove noise employs multiresolution transformations that convert chaotic signals between the temporal plane to the video frames. Forget the overall transformation function for information, we eliminated those harmonic components of disturbance from all levels. The computation effectiveness and the segmented result's dependability are both enhanced in this manner.

Convolutional neuronal systems were used in our research. One convolutional plane plus the nonlinear system levels are the 2 kinds of strands in a CNN. Following mixture, each permutation level generates several characteristic mappings. To obtain the information mapping for these pooled layers, individual units of each grouping in the featured mapping are changed by applying weights and delay, as well as a polynomial kernel. In comparison to manually and automated categorization, researchers were capable can achieve better precise outcomes in less effort using several convolutional and pooled levels. We then employed simultaneous computation to speed up the

operation even yet even farther. This maestro paradigm was implemented by designating 1 network as the network, which is in charge of overall information partitioning and assignment while assigning other networks to perform regional information calculations and send the results to the mistress device.

That information was gathered through elevated cryosection color photographs of an older male standard. It contains different cells and a preserved upright male chest, including exact prefrontal cortical folded architecture. It provided us with an averaged proportion of every cerebral cell. Our results have a margin of error of less than 2.21 percent. Some other useful metric is the GM/WM ratios, that aids in the assessment of specific cerebral pathologies. With a correctness ratio of up to 95%, our outcome is likewise extremely pleasing. Every one of the five people's minds in our collection has 160 pictures. The outcomes are persuasive. They could not examine the precision on their border against previous research because their effort focuses on overall proportion across the organs. They shall concentrate our future study on comparing the border and employ datasets through Brain Net, an internet platform that delivers 3D Magnetic resonance brains information. It gives consumers flexible modeling to determine the portion capacity and is an excellent approach to check our product's correctness.

There are several drawbacks to our investigation. Initially and foremost, due to a lack of resources, our database is not particularly huge. Throughout the hereafter, we will enhance both the amount and diversity of the examples, incorporating persons of various colors such as black, white, and yellow. We'll additionally require specimens for people of all generations, including infants, adolescents, and the geriatric. Now, our database solely contains grownups. We can identify the specimens by age, gender, race, and other factors with a larger database. We want to establish a judgment threshold for healthcare diagnosis. Investigators and physicians may contrast the participant's brain's information to their information to validate an aberrant percentage of structures in the brain and subsequently identify the condition.

Test case

Decrease overall duration by using concurrent processing. This maestro paradigm is used. Its block, which oversees information division and assignment, is one of the nodes. Then additional networks finish the localized information calculations and send the outcome to the supervisor cluster. Whenever dealing with enormous

amounts of information, this is critical. Because of the information quantity constraint, my finding is hardly meaningful. The stronger that answer produced, the greater the database. **Figure 9** depicts a graphic representation of the temporal frequency.

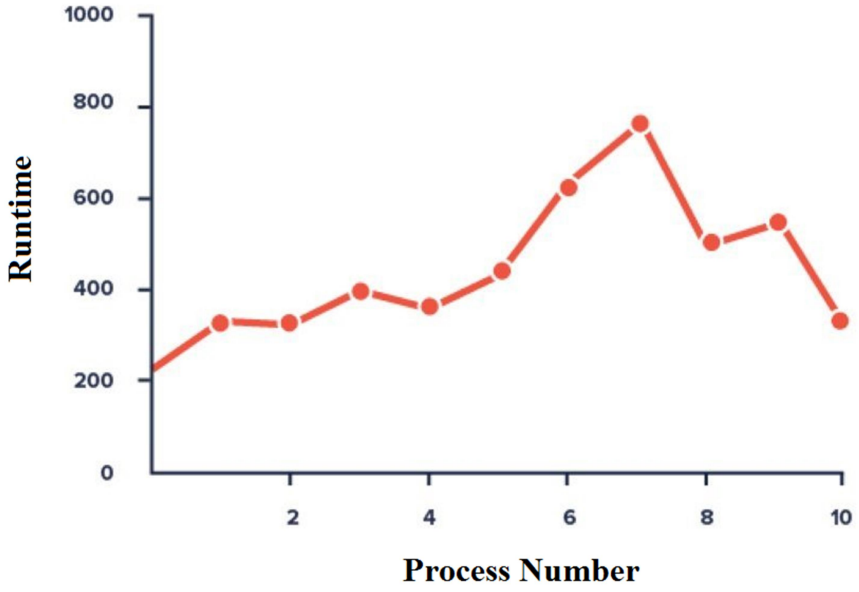

Figure 9: Runtime Vs Process Number

CONCLUSION

Finally, we demonstrated how to use a multilayer neuronal network to efficiently separate cerebral regions with MRI images. The percentages are extremely like the VCH female's median adult cerebral statistics. Because computer technology and machines understanding had become greater extensively implemented in the investigation, this is a milestone. Overall efficiency or efficiency of therapeutics can be enhanced by incorporating deeper training. This is due to computers can evaluate information continuously, making it speedier and more effective than human or automated examination. Researchers may view the outlines of the boundaries between various organs throughout 3D for prospective study, which can then be combined with optically modeling tools like MCVM for decreased laser treatment. This research has a lot more promise in the medicinal area, and therefore believe this approach may be used as a diagnostic criterion.

REFERENCES

[1] Ismael SA, Mohammed A, Hefny H. An enhanced deep learning approach for brain cancer MRI images classification using residual networks. Artificial intelligence in medicine. 2020 Jan 1;102:101779.

[2] Lu Z, Zhan X, Wu Y, Cheng J, Shao W, Ni D, Han Z, Zhang J,

Feng Q, Huang K. BrcaSeg: A Deep Learning Approach for Tissue Quantification and Genomic Correlations of Histopathological Images. Genomics, Proteomics & Bioinformatics. 2021 Jul 17.

[3] Shen Z, Li W, Han H. Deep Learning-Based Wavelet Threshold Function Optimization on Noise Reduction in Ultrasound Images. Scientific Programming. 2021 Aug 26;2021.

[4] Nowak S, Faron A, Luetkens JA, Geißler HL, Praktiknjo M, Block W, Thomas D, Sprinkart AM. Fully automated segmentation of connective tissue compartments for CT-based body composition analysis: A deep learning approach. Investigative radiology. 2020 Jun 1;55(6):357-66.

[5] Kader IA, Xu G, Shuai Z, Saminu S, Javaid I, Ahmad IS, Kamhi S. Brain Tumor Detection and Classification on MR Images by a Deep Wavelet Auto-Encoder Model. Diagnostics. 2021 Sep;11(9):1589.

[6] Juneja M, Saini SK, Kaul S, Acharjee R, Thakur N, Jindal P. Denoising of magnetic resonance imaging using Bayes shrinkage based fused wavelet transform and autoencoder based deep learning approach. Biomedical Signal Processing and Control. 2021 Aug 1;69:102844.

[7] Kader IA, Xu G, Shuai Z, Saminu S, Javaid I, Ahmad IS, Kamhi S. Brain Tumor Detection and Classification on MR Images by a Deep Wavelet Auto-Encoder Model. Diagnostics. 2021 Sep;11(9):1589.

[8] Sarhan AM. Brain tumor classification in magnetic resonance images using deep learning and wavelet transform. Journal of Biomedical Science and Engineering. 2020 Jun 17;13(06):102.

[9] Latchoumi, T. P., Balamurugan, K., Dinesh, K., & Ezhilarasi, T. P. (2019). Particle swarm optimization approach for waterjet cavitation peening. *Measurement*, *141*, 184-189.

[10] Singh Y, Shakyawar D, Hu W. An Automated Method for Detecting the Scar Tissue in the Left Ventricular Endocardial Wall Using Deep Learning Approach. Current medical imaging. 2020 Mar 1;16(3):206-13.

[11] Qu L, Zhang Y, Wang S, Yap PT, Shen D. Synthesized 7T MRI from

3T MRI via deep learning in spatial and wavelet domains. Medical image analysis. 2020 May 1;62:101663.

[12] Masud M, Sikder N, Nahid AA, Bairagi AK, AlZain MA. A machine learning approach to diagnosing lung and colon cancer using a deep learning-based classification framework. Sensors. 2021 Jan;21(3):748.

[13] Çinarer G, Emiroğlu BG, Yurttakal AH. Prediction of Glioma Grades Using Deep Learning with Wavelet Radiomic Features. Applied Sciences. 2020 Jan;10(18):6296.

[14] Arab A, Chinda B, Medvedev G, Siu W, Guo H, Gu T, Moreno S, Hamarneh G, Ester M, Song X. A fast and fully-automated deep-learning approach for accurate hemorrhage segmentation and volume quantification in non-contrast whole-head CT. Scientific Reports. 2020 Nov 9;10(1):1-2.

[15] Paladini E, Vantaggiato E, Bougourzi F, Distante C, Hadid A, Taleb-Ahmed A. Two Ensemble-CNN Approaches for Colorectal Cancer Tissue Type Classification. Journal of Imaging. 2021 Mar;7(3):51.

[16] Javaheri T, Homayounfar M, Amoozgar Z, Reiazi R, Homayounieh F, Abbas E, Laali A, Radmard AR, Gharib MH, Mousavi SA, Ghaemi O. Covidctnet: An open-source deep learning approach to identify covid-19 using ct image. arXiv preprint arXiv:2005.03059. 2020 May 6.

[17] Masud M, Sikder N, Nahid AA, Bairagi AK, AlZain MA. A machine learning approach to diagnosing lung and colon cancer using a deep learning-based classification framework. Sensors. 2021 Jan;21(3):748.

[18] Shen SC, Fernández MP, Tozzi G, Buehler MJ. Deep learning approach to assess damage mechanics of bone tissue. Journal of the Mechanical Behavior of Biomedical Materials. 2021 Nov 1;123:104761.